Polycube Shape Space

Hui Zhao [1,2] [†] Xuan Li [4] [‡] Wencheng Wang [1,2] [§] Xiaoling Wang [3] Shaodong Wang [1,2] Na Lei [5] [¶] Xiangfeng Gu [4]

[1] State Key Laboratory of Computer Science, Institute of Software, Chinese Academy of Sciences
[2] University of Chinese Academy of Sciences [3] University of Science and Technology Beijing, China
[4] State University of New York at Stony Brook, USA [5] Dalian University of Technology, China
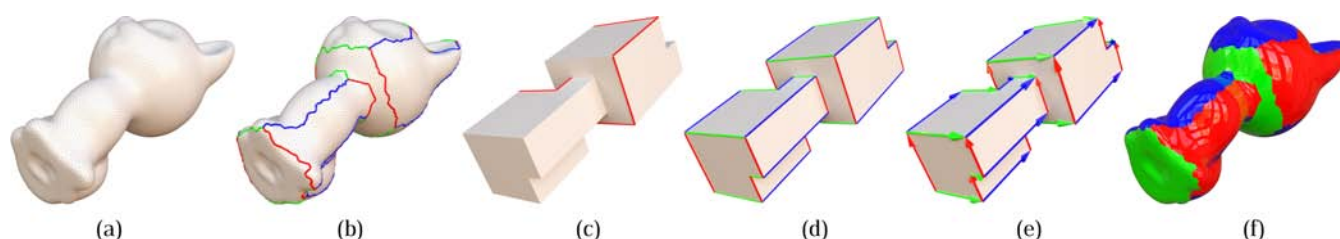
Figure 1: *(a) the "kitten" mesh of genus one, (b) the polycube graph, (c) the homology loops, (d) the arc colorization, (e) the initial directions, (f) the polycube topology.*

Abstract

There are many methods proposed for generating polycube polyhedrons, but it lacks the study about the possibility of generating polycube polyhedrons. In this paper, we prove a theorem for characterizing the necessary condition for the skeleton graph of a polycube polyhedron, by which Steinitz's theorem for convex polyhedra and Eppstein's theorem for simple orthogonal polyhedra are generalized to polycube polyhedra of any genus and with non-simply connected faces. Based on our theorem, we present a faster linear algorithm to determine the dimensions of the polycube shape space for a valid graph, for all its possible polycube polyhedrons. We also propose a quadratic optimization method to generate embedding polycube polyhedrons with interactive assistance. Finally, we provide a graph-based framework for polycube mesh generation, quadrangulation, and all-hex meshing to demonstrate the utility and applicability of our approach.

CCS Concepts

• Mathematics of computing → Graphs and surfaces; • Computing methodologies → Mesh models; Mesh geometry models;

1. Introduction

The relationship between a graph and a polyhedron is a crucial and challenging problem. However, there are few of attempts on it. Steinitz's theorem [Zie12; GKKZ67] establishes a bi-directional relationship between a graph and a convex polyhedron in $\mathbb{R}^3$ by the statements that "a graph is the skeleton graph of a convex polyhedron if and only if it is 3-connected and planar." Branko Grünbaum call it "the most important and deepest known result on 3-polytopes" [GKKZ67].

A *k*-connected graph remains connected when few than *k* vertices are removed. A planar graph can be embedded in the plane. If each vertex has *k* neighbors, it is called a k-regular graph. A bipartite graph is a graph whose vertices can be divided into two disjoint and independent groups, a bipartite graph does not have odd-length cycles.

Steinitz's theorem works only for convex polyhedra. Eppstein et al. [EM10] propose an analogous theorem for a special kind of non-convex polyhedra named *simple orthogonal polyhedra*, which satisfies three requirements: 1) the sphere topology, 2) simply connected faces, 3) exactly three mutually-perpendicular axis-parallel edges meeting at every vertex. Eppstein's theorem states "a graph is the skeleton graph of a *simple orthogonal polyhedron* if and only if it is bipartite, planar, 3-regular and removal of any 2 of its vertices disconnects it into at most 2 components." Furthermore, based on

[†] alanzhaohui@qq.com
[‡] xuanli2@cs.stonybrook.edu
[§] whn@ios.ac.cn, corresponding author
[¶] nalei@dlut.edu.cn, corresponding author

these characterizations of *simple orthogonal polyhedra*, Eppstein et al. [EM10] present a linear algorithm to construct a *simple orthogonal polyhedron* from a valid graph.

Simple orthogonal polyhedra is a special kind of well-known *polycube polyhedron* in the graphics community, whose every face is perpendicular to one of the coordinate axes. In this paper, we prove a theorem that generalizes Steinitz's and Eppstein's theorems for a broader class of *polycube polyhedra* with any genus, non-simply connected faces, but we also require that three edges meeting at every vertex (Note that there are polycubes whose vertex has more than three edges). Our theorem states that " a *polycube graph* (3.1) is a skeleton graph of a *polycube polyhedron* (3.2) if the patch number of the graph is bigger than 3." Based on our framework, we further design a linear system to build a space of *polycube polyhedra* from the corresponding graph. Our approach is flexible to adjust the geometry of a *polycube polyhedron*. In summary, given a graph, our theorem addresses the following problem: 1) the existence of the polycube polyhedron; 2) the dimension of polycube shape space; 3) the method to generate the polycube polyhedron.

Polycube mesh (or polycube) plays an important role in graphics research. Polycube is firstly proposed in [THCM04] to extend cube mapping to general shapes. Polycube has a highly regular structure and a special global parametric domain. It is a special geometric shape that all face normals are aligned with one axis of a specific orthonormal coordinate frame. Polycube removes the detail of the original meshes and captures its global features. It has been used in many kinds of graphics applications, such as: surface texturing [THCM04], volumetric texturing [CL*10], parameterization [GXH*13], reconstruction [WJH*08], shape morphing[FJFS05] and T-mesh construction [LZLW15]. Many algorithms of hexahedral remeshing [GSZ11; HXH10; LVS*13; HJS*14; FBL16] also rely on *polycube mesh* heavily. Usually, they generate a corresponding *polycube mesh* from the original shape by deformation, the difficult hexahedral meshing operation is transferred onto the *polycube mesh*.
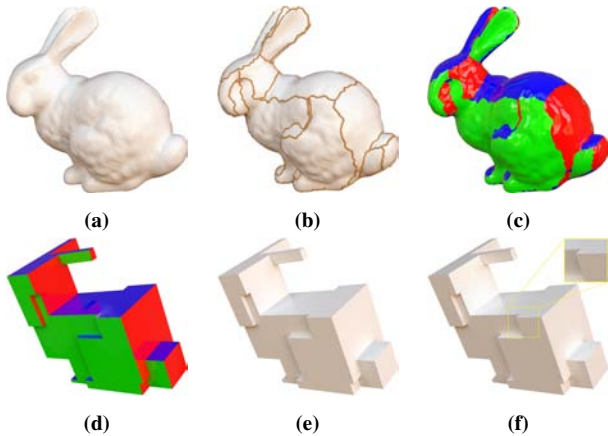

Figure 2: *(a) the original mesh; (b) the* polycube graph *embedded on the mesh; all patches are colored according to their orientations (c),(d); the* polycube polyhedron *(e); the* polycube mesh *(f).*

Currently, there are two major frameworks in quadrangula-

tion and all-hex meshing: *deformation based* [FBL16; HJS*14; LVS*13; GSZ11] and *frame-field based* [NRP11; HTWB11; LLX*12; JHW*14; LBK16]. By the relationship between a graph and a *polycube polyhedron*, we provide a *graph-based* framework for the quadrangulation and all-hex meshing applications. Our framework works as follows: given an input graph embedded in a mesh, first, we build a *polycube polyhedron*, then we map the original mesh onto it to achieve a *polycube mesh*, which can be used in quadrangulation and all-hex meshing.

Contribution. Our major contribution is proving a theorem which characterizes the relationship between a graph and a *polycube polyhedron*, our theorem provides a necessary condition for the skeleton graph of a *polycube polyhedron*. Our second contribution is to design a linear system to realize a set of adjustable *polycube polyhedra* for a valid graph. Our third contribution is presenting a graph-based framework for the applications of *polycube mesh* generation, quadrangulation, and all-hex meshing, as demonstrated in Fig. 2b.

The organization of the paper is: Section 2 summarizes the relevant works; the concepts are introduced in Section 3; *polycube shape space* is explained in Section 4; the embedding is detailed in Section 5; finally the applications of quadrangulation and all-hex meshing are illustrated in Section 6.

2. Related Works

The most related work to ours is Steinitz's theorem [Zie12; GKKZ67] and Eppstein's theorem [EM10]. Our *polycube shape space* is also motivated by the applications of polycube generation, mesh parameterization, quadrangulation, all-hex meshing. Because of the abundance of literature, we will focus only on the ones which are directly relevant to ours.

In two dimensions, a graph is a skeleton graph of a polytope if and only if it is a cycle. In three dimensions, Steinitz's theorem addresses what kind of graph can be the skeleton graph of a convex polyhedron. The sufficient and necessary condition between a graph and a general non-convex polyhedron is still unknown. For convex polyhedra with all vertices on a sphere, the graph-theoretic characterizations are discussed in [DS96; HRS92; Riv96]. For non-convex polyhedra with star-shaped faces, and all but one face are visible from a common viewpoint, the characterizations are addressed in [Hon08].

Two special cases of *simple orthogonal polyhedron* : *corner polyhedron* and *xyz polyhedron* are investigated in [EM10] (see [EM10, Fig. 1]). If all but three faces of a *simple orthogonal polyhedron* are oriented towards the vector, it is called *corner polyhedron*. If each axis-parallel line of a *simple orthogonal polyhedron* has at most two vertices, it is called *xyz polyhedron*. A *corner polyhedron* is always an *xyz polyhedron*. Eppstein et al. [EM10] prove the following theorems:

Theorem 2.1 ([EM10]) A graph is the skeleton graph of a corner polyhedron if and only if it is planar, bipartite, 3-regular and its dual is 4-connected.

Theorem 2.2 ([EM10]) A graph is the skeleton graph of an *xyz* polyhedron if and only if it is planar, bipartite, 3-regular and 3-connected.

A *simple orthogonal polyhedron* can be divided into *xyz polyhedrons*, which furthermore is separated into *corner polyhedrons*. Their induction proof also gives an efficient linear time algorithm to construct the *simple orthogonal polyhedron* for a given graph. While Steinitz's and Eppstein's statements are remarkable, it is limited to a small class of polyhedra, our approach can address and construct more polyhedra.

In the graphics community, *polycubes* are constructed from not graphs, but meshes. The methods in [THCM04; YL08] construct *polycube* manually, then another extracting step is applied to achieve the cross-surface mapping between the mesh and its polycube shape [WJH*08]. The method in [LJFW08] uses segmentation and box-primitives to approximate original models, but it fails on complicated meshes. A divide-and-conquer algorithm is applied in [HWFQ09], however, it generates over-refined polycubes. Both of [HWFQ09; LJFW08] can not build the cross-surface mapping automatically.

The deformation based approaches in [GSZ11; HJS*14; FBL16] obtain *polycube meshes* by minimizing an energy. Given a surface and a valid *polycube topology*, Zhao et al. [ZLL*18] propose a novel method to deform a mesh into its *polycube mesh* by rotating face normals. The algorithm in [GSZ11] uses a rotation-driven method to align each surface normal to one direction of $(\pm X, \pm Y, \pm Z)$ gradually; then a position-driven deformation is used to enforce the planarity and straightness. Based on the observation that every face normal of a *polycube* is aligned with one axis and the value of the ℓ_1-norm of every unit face normal is equal to 1, Huang et al. [HJS*14] propose a ℓ_1-norm energy weighted by triangle areas and a variational method to generate *polycube meshes*. However, their system is nonlinear and the results are affected by the orientation of the mesh. They need another energy to find an optimal global orientation and a post-processing cleanup step to fix spurious topological degeneracy.

The graph-cut based approach [LVS*13] balances the parameterization distortion and the number of singularities of polycube vertice. Fu et al. [FBL16] propose another face normal-rotation method to deform a mesh into a *polycube mesh*. A method proposed in [CLS16] simplifies the complicated polycube topology. A special method that extends polycubes and parameterizes a mesh with more than one chart is proposed in [FXBH16]. However, this method is designed for all-hex meshing directly, and can not produce a *polycube mesh*.

Frame-field based hexahedral mesh generation is applied in [HTWB11; JHW*14; LBK16], which has internal singularities and can not guarantee a valid singularity structure. Polycube based hexahedralization can produce a special kind of hexahedral mesh which has no internal singularity [GSZ11; HJS*14; LVS*13; FXBH16]. These mesh-based methods normally generate one single *polycube mesh*, instead, our graph-based one can obtain a set of results by embedding a graph on the mesh. Analyzing and optimizing the polycube structure by a graph is also studied in [CXW*19].

3. Background

3.1. Basic Concepts

In this paper, we distinguish the concepts of *polycube polyhedron* and *polycube mesh*. A *polycube polyhedron* is a polyhedron with planar orthogonal polygonal faces (Fig. 2e). A *polycube mesh* has the same overall shape with its corresponding polycube polyhedron, but every planar polygonal face is triangulated (Fig. 2f). We call a layout graph on a mesh as a *polycube graph* if it can lead to a valid *polycube topology* (Fig. 2b). If all patches of a mesh separated by a layout graph can be assigned a valid set of coordinate axis labels (as shown in Fig. 2c and 2e, the red, green and blue colors represent the labels of X, Y, Z axis respectively), we call this assignment a valid *polycube topology*,

Definition 3.1 A layout graph is called a *polycube graph* $G = (N, A, P)$ with the nodes N, the arcs A and the patches P, if it satisfies two conditions: 1) each node $n_i \in N$ is of valence 3, i.e. there are 3 arcs incident to it; 2) each patch $p_i \in P$ has an even valence, i.e. there are even number of nodes along the border of each patch.

A *polycube graph* is 3-regular. A patch corresponds to a graph cycle. In this paper, we only discuss a special subset of all valid polycubes in general sense. For example, the red node of the polycube in Fig. 3a has valance 4, therefore this layout graph does not satisfy our requirements. However, we can always modify this kind of graph to be valid, then generate a similar polycube (Fig.3b). Note that If each patch is of valence 4, then it is called *quad layout graph* [CK14].
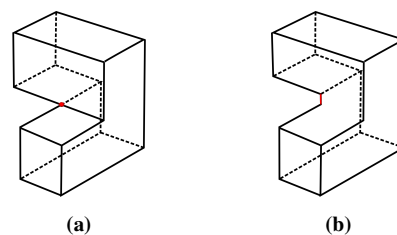
Figure 3: *(a) A polycube that violates our requirements; (b) modified valid version.*

Definition 3.2 A *polycube polyhedron* is a three-dimensional polyhedron (not necessarily convex) which has exactly three mutually-perpendicular axis-parallel edges meeting at every vertex.

The vertices, edges, faces of a *polycube polyhedron* correspond to the nodes, arcs, patches of a *polycube graph*. The surface normals of a *polycube polyhedron* are axis-aligned and each face is perpendicular to one coordinate axis. Note that a valid *polycube graph* may lead to an invalid *polycube polyhedron*. For example, in Fig. 4, the *polycube graph* is valid, however, the heights of the two red edges in the vertical direction are 0, the polyhedron is not valid.

Definition 3.3 If a *polycube graph* has an embedding in $\mathbb{R}^3$ to form a *polycube polyhedron*, such an embedding is called a *polycube embedding* of the polycube graph.

When a *polycube graph* G is embedded in a mesh M, each node n_i, each arc a_i of G are mapped to a vertex v_i and a chain of edges $C_i = \{e_1, e_2, \ldots, e_n\}$ of mesh M respectively (Fig. 5). A mesh can have many different embedded *polycube graphs* (Fig. 6).
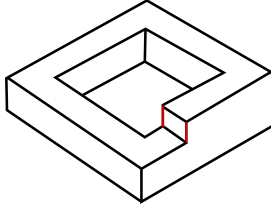
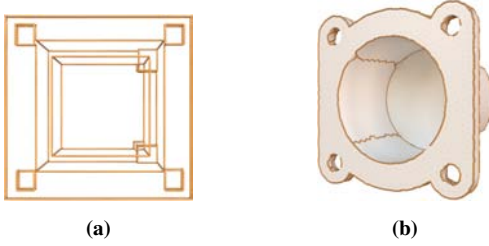**Figure 4:** *A valid polycube graph maybe leads to an invalid polyhedron (the height of two red edges are* 0*).*

(a)   **(b)**

Figure 5: *A* polycube graph *embedding in* $\mathbb{R}^3$ *(a) and an embedding on a mesh (b).*

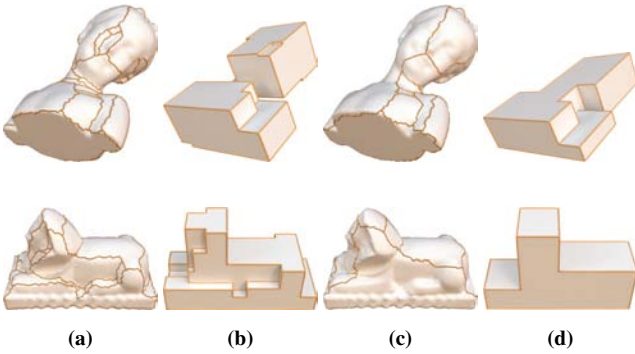**(a)**   **(b)**   **(c)**   **(d)**

Figure 6: *The different* polycube graphs *(a) (c) embedded on the same mesh and their corresponding* polycube polyhedra *(b) (d).*

3.2. The Characteristics of Polycube Polyhedra

A *polycube polyhedron* is also called an orthogonal polyhedron [LVS*13; EM10]. It can have any kind of genus. The faces on a *polycube polyhedron* can be simply or non-simply connected. A simply connected face is of disk-topology, while a non-simply connected face has some holes inside it (Fig. 7).
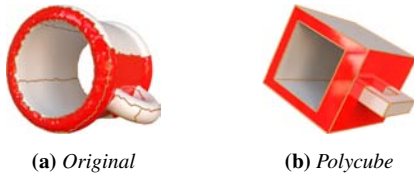

(a) *Original*   **(b)** *Polycube*

Figure 7: *The non-simply connected faces (red) on a model and on the corresponding* polycube polyhedron.

A *polycube polyhedron* itself is a 2-dimensional manifold. Its

skeleton determines a unique polycube graph. However, for a *polycube graph*, the corresponding *polycube polyhedron* is not unique, as shown in Fig. 8.
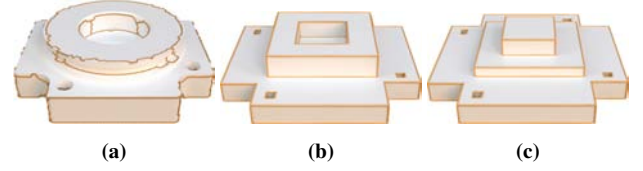

(a)   **(b)**   **(c)**

Figure 8: *Two different* polycube polyhedra *(b), (c) correspond to the same* polycube graph *(a).*

The Gaussian curvature s_i of any vertex i of a *polycube polyhedron* has only two options: $+\frac{\pi}{2}$ (the white vertices in Fig. 9 and Fig. 10) and $-\frac{\pi}{2}$ (the black vertices). The sum of all Gaussian curvatures must satisfy the Gauss-Bonnet theorem: $\sum s_i = 2\pi(2 - 2g)$, where g represents the genus. Some geometric information of a *polycube polyhedron* can be determined by the combinational features of the *polycube graph*. If three neighboring patches of one node of a *polycube graph* are all of valence 4, then the Gaussian curvature of the corresponding vertex on the *polycube polyhedron* must be $+\frac{\pi}{2}$ (the black vertices in the red circle of Fig. 9).
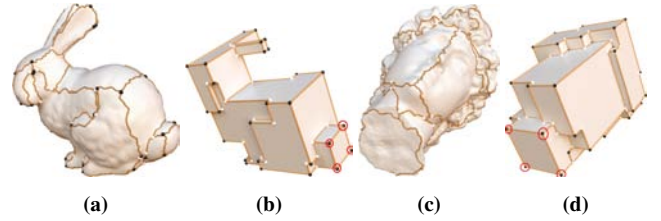

(a)   **(b)**   **(c)**   **(d)**

Figure 9: *The pre-determined Gaussian curvatures.*

For a *polycube polyhedraon* of genus zero, the difference between the numbers of vertices with Gaussian curvature $+\frac{\pi}{2}$ and $-\frac{\pi}{2}$ is eight; for a *polycube polyhedraon* of genus one, the two groups have the same number of vertices.

For a non-simply connected face of a *polycube polyhedron*, there are more than one arc loops in the corresponding *polycube graph*. If an inner arc loop consists of four arcs, then the Gaussian curvatures of the vertices on this inner arc loop are all $-\frac{\pi}{2}$; if an outer arc loop consists of four arcs, then the Gaussian curvatures of the vertices are all $+\frac{\pi}{2}$. For example, the white vertices $(-\frac{\pi}{2})$ and the black vertices $(+\frac{\pi}{2})$ in Fig. 10. In fact, all Gaussian curvatures of the vertices can be pre-determined in Fig. 10. However, a *polycube graph* corresponds to many different *polycube polyhedra*, its combinational structure cannot determine all Gaussian curvatures.

4. Polycube Shape Space

In this section, we present an algorithm to construct a vector space of *polycube polyhedron* from a *polycube graph* and prove the necessary condition for the skeleton graph of a *polycube polyhedron*.
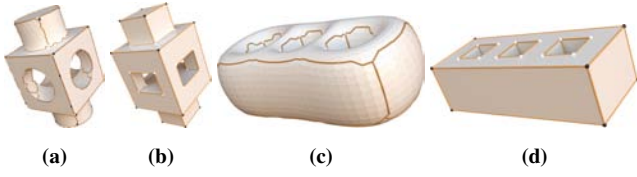
Figure 10: *The pre-determined Gaussian curvatures on the non-simply connected faces.*

4.1. Arc Colorization

We observe that a *polycube polyhedron* has two crucial properties: 1) the directions of all edges on one face f_i must switch between two axes of d_1, d_2; 2) the normal of the face f_i must point to the third axis of d_3. Based on these observations, we design an arc colorization algorithm to assign axis labels to all arcs of a *polycube graph*, such that we can determine the coordinate axes for the edges and the faces of its corresponding *polycube polyhedron* accordingly. Note that the color label on an arc indicates its axis, it can not distinguish the positive or the negative directions of the axis.
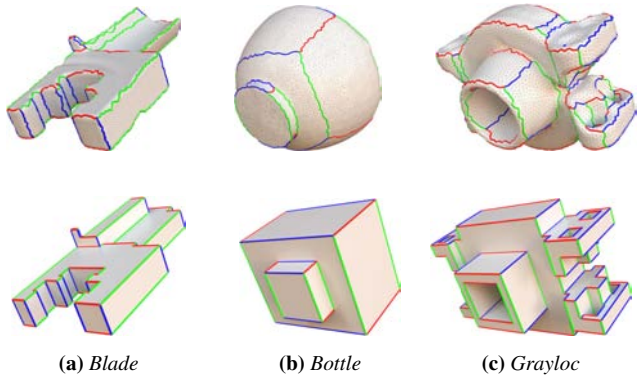

(a) *Blade*   **(b)** *Bottle*   **(c)** *Grayloc*

Figure 11: *The colorized arcs. The arcs of a* polycube graph *are curve lines, for better visualization, we draw them by straight lines on a* virtual polycube polyhedron.

Let red, blue, green colors represent the X, Y, Z coordinates respectively. First, we start from a node of the *polycube graph G* and assign three colors to its three neighboring arcs; then our algorithm travels the whole *polycube graph* patch by patch with a breadth-first method and colorizes the arcs of every patch by switching between two corresponding colors. Some colorized *polycube graphs* are exhibited in Fig. 11. The pseudocode is shown in Alg. 1.

Three colors have six permutations, which leads to six different colorizations for a *polycube graph*. However, all of them are equivalent under rotation and reflection transformations. Any permutation can be our input for the next step.

4.2. Differential One-Form

A *polycube embedding* induces a natural vector valued differential one-form and differential 0-form on a *polycube graph*. First, we define an edge length function L on all arcs A of a *polycube*

ALGORITHM 1: Arc Colorization

Input: A polycube graph $G = (N, A, P)$
Output: A 3-colorization of the arc set A

   1. Choose a root patch p_0 in P and colorize its arcs using two different colors alternatively.

for *each node n_j of patch p_0* **do**
   | 2. Use the left one color to colorize the left one arc at n_j that is not colorized
end

for *p_i in the breadth-first sequence of P from p_0* **do**
   | 3. Traverse along arcs of p_i, assume colors have been used are c_1 and c_2.
   | 4. Colorize left arcs of p_i using c_1, c_2 such that colorization is an alternative pattern.
   | 5. **for** *each node n_j of patch p_i* **do**
   | | Use color c_3 to colorize the left one arc at n_j that is not colorized
   | **end**
end

return *3-colorized polycube graph G*.

---

graph as: $L : A \rightarrow \mathbb{R}$. Second we define a positive orientation on A: $d : A \rightarrow \{\mathbf{e}_1, \mathbf{e}_2, \mathbf{e}_3\}$, where $\mathbf{e}_1, \mathbf{e}_2, \mathbf{e}_3$ is the standard basis of $\mathbb{R}^3$. Then we propose a vector-valued differential one-form on the *polycube graph G* as: $\omega = L * d$, where "$*$" is the scalar product. The exterior derivative of ω is a 2-form on the patch set P: $d\omega(p_i) = \sum_{a_j \in p_i} \omega(a_j)$, here a_j is the boundary arcs of the patch p_i. The integration of ω on a directed arc chain γ_i is defined as: $\int_{\gamma_i} \omega = \sum_{a_j \in \gamma_i} \omega(a_j)$.

For a *polycube polyhedron* embedded in $\mathbb{R}^3$, the total sums of the edge length vectors on every loop of the *polycube polyhedron* are 0. It means the differential one-form ω is *closed* and *exact*. A *closed* differential one-form ω satisfies:

$$d\omega = \mathbf{0}. \tag{1}$$

The integration of an *exact* differential one-form on any closed loop is 0, it is equivalent to that the integration is 0 on every homology basis of the homolopy group $H(G)$ of a *polycube graph G*:

$$\int_{\gamma_i} \omega = 0, \quad \forall \gamma_i \in H(G), \tag{2}$$

Accordingly, we can compute a vector valued differential 0-form V_ω on the nodes N of the *polycube graph G* by integrating this differential one-form, such that the differential 0-form V_ω determines the vertex positions of the corresponding *polycube polyhedron*:

$$V_\omega : N \rightarrow \mathbb{R}^3.$$

We pick up any node n_0 as the root and set its position to be $(0,0,0)$, then the position of any other node n_i can be integrated as:

$$V_\omega(n_i) = \int_{\gamma(n_0, n_i)} \omega,$$

where $\gamma(n_0, n_i)$ is an arc chain from n_0 to n_i.

4.3. Linear System

The differential one-form ω consists of two parts: L and d, the axis of d of each arc is already computed by the colorization. We can

randomly choose a positive direction for d (Fig. 12). The variable L_i may be negative, which means that the corresponding edge has the opposite direction to this initial assignment.
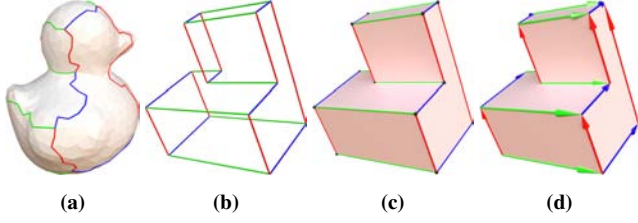

(a)   **(b)**   **(c)**   **(d)**

Figure 12: *The colorized arcs are shown in (a), (b), (c), and the initial directions are exhibited in (d).*

If a patch has more than one boundary, it is a non-simply connected patch (Fig. 13a), we need to pre-process them to be simply connected (Fig. 13b) by splitting the arcs and adding more arcs. Note that the newly added patches may not be able to embed in $\mathbb{R}^3$. But the splitting will not affect the positions of original nodes, i.e., the embedding of the original *polycube graph*. The pseudocode is detailed in Alg. 2.
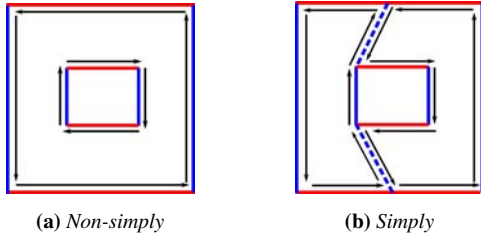

(a) *Non-simply*   **(b)** *Simply*

Figure 13: *The non-simply connected patch (a); the modified simply connected patch (b).*

The added edges are just logical connection which guarantees that all vertices are connected (by real edges or virtual edges). This is helpful for colorization and linear system construction. The final embedding only includes real edges (the edges before splitting). We can imagine these connections as free ropes that connect the inner holes to the outside boundary. They can freely move along the boundary.

For each patch p_j, the equation is of the form:

$$d\omega(p_j) = \sum_{a_i \in p_j} (L_i \cdot d_i) = 0. \tag{3}$$

If the genus of the mesh is not zero, i.e., the genus of its embedding *polycube graph* is not zero. For each homomogy basis loop γ_j (Fig. 14 and Fig. 15) in its homology group $H(G)$, the equation is of the following form:

$$\int_{\gamma_j} \omega = \sum_{a_i \in \gamma_j} (L_i \cdot d_i) = 0. \tag{4}$$

Eqn. 3 and 4 in combination can be expressed as a linear system:

$$W \cdot L = 0 \tag{5}$$

ALGORITHM 2: Non-simply connected patches

Input: A polycube layout $G = (V, A, P)$ with some non-simply connected faces

Output: New polycube layout $G' = (V', A', P')$ without non-simply connected patches

for p_i *in the set of non-simply connected faces* **do**
  1. Assume p_i is colorized by color c_1 and c_2. Find two arcs a_1, a_2 colorized by c_1 in outer boundary of p.
  2. Get all inner holes of p_i: $h_1, h_2, ..., h_n$.
  for $i \leftarrow 1$ *to* n **do**
    3. Find an arc in h_i colorized by c_2. Assume its end vertices are v_1, v_2.
    4. Add a vertex v_{1i} to a_1, v_{2i} to a_2.
    5. Add an arc between v_1 and v_{1i}, an arc between v_2 and v_{2i}.
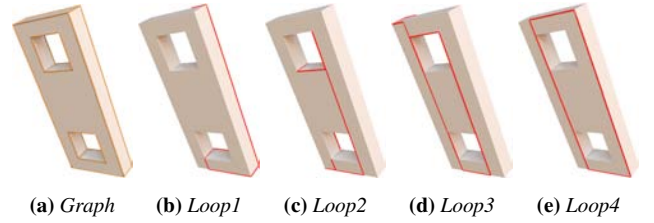 **end**
end
return *New polycube graph G'.*

(a) *Graph*   **(b)** *Loop1*   **(c)** *Loop2*   **(d)** *Loop3*   **(e)** *Loop4*

Figure 14: *The four homology basis loops (red lines) of the "double torus" model.*

(a) *Graph*   **(b)** *Loop1*   **(c)** *Loop2*   **(d)** *Loop3*   **(e)** *Loop4*
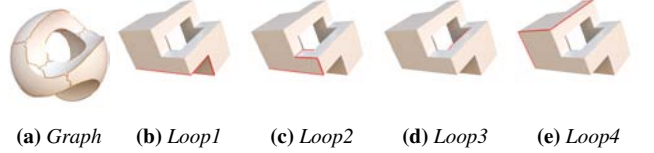
Figure 15: *The four homology basis loops (red lines) of the "sculpt" model are illustrated on the virtual polycubes.*

4.4. Kernel Space

If the dimension of the kernel space K of the matrix W is zero, it means that there is no valid *polycube polyhedron*. We define the kernel space of the matrix W as the *polycube shape space* of the corresponding *polycube graph*. The basis of the kernel space forms the basis of the *polycube shape space*, as shown in Fig. 16. We generalize the Eppstein's result [EM10] by the following theorem.

Theorem 4.1 If a polycube graph can realize a polycube polyhedron embedded in $\mathbb{R}^3$, then the dimension of the corresponding kernel space K is not zero.

This is a necessary condition, some elements in the *polycube shape space* cannot lead to a valid *polycube embedding*.

We denote the numbers of nodes, arcs and patches of a polycube graph layout as $|N|$, $|A|$, $|P|$. After arc splitting, these three quantities become $|N'|$, $|A'|$, $|P'|$. Assume there are k inner loops in all

Table 1: *The dimension of polycube shape spaces*

Model	$|N|$	$|A|$	$|P|$	$|N'|$	$|A'|$	$|P'|$	genus	dimension
airplane	52	78	28	52	78	28	0	25
armadillo	236	354	120	236	354	120	0	117
armchair	24	36	14	24	36	14	0	11
bimba	68	102	38	72	110	40	0	35
bone	40	60	22	40	60	22	0	19
bunny	84	126	44	84	126	44	0	41
coverrear	72	108	44	84	132	50	0	41
david	90	135	47	90	135	47	0	44
dente	44	66	24	44	66	24	0	21
dino2	106	159	55	106	159	55	0	52
hand	48	72	26	48	72	26	0	23
max	64	96	35	66	100	36	0	32
pear	24	36	16	28	44	18	0	13
pensatore	136	204	70	136	204	70	0	67
sphinx	72	108	38	72	108	38	0	35
bottle	52	78	29	58	90	32	1	26
camel	284	426	144	288	434	146	1	141
dragon	210	315	105	210	315	105	1	102
kitten	46	69	24	48	73	25	1	21
rocker	66	99	36	72	111	39	1	33
teaport	48	72	28	56	88	32	1	25
cup	32	48	18	40	64	22	2	15
dtorus	40	60	22	48	76	26	2	19
eight	24	36	14	32	52	18	2	11
sculpt	40	60	18	40	60	18	2	15
block	48	72	26	60	96	32	3	23
elephant	176	264	85	178	268	86	3	82
holes3	32	48	18	44	72	24	3	15
kiss	146	219	70	148	223	71	3	67
Deckel	80	120	40	92	144	46	4	37
fertility	104	156	46	104	156	46	4	43
sculpture	108	162	51	114	174	54	4	48
botijo	154	231	71	158	239	73	5	68
dancing	216	324	101	230	352	108	8	98

non-simply connected patches. One observation is:

$$|N'| = |N| + 2k$$
$$|A'| = |A| + 4k \qquad (6)$$
$$|P'| = |P| + k$$

We induce the following theorem for the dimension of *polycube shape space*. The experimental statistics are shown in Table 1.

Theorem 4.2 For a polycube graph with the number of nodes $|N|$, arcs $|A|$, patches $|P|$ respectively, the dimension of its polycube shape space is at least $|P| - 3$.

PROOF. By Euler's polyhedron formula,

$$|N'| - |A'| + |P'| = 2 - 2g. \qquad (7)$$

There are three arcs for every node of a *polycube graph*, so we have

$$3|N| = 2|A|, \qquad (8)$$

By Equation 6 and the two equations above, we get

$$|A| = 3|P| - 3k - 6 + 6g \qquad (9)$$

Every patch (before adding auxiliary arcs) at most provides 2 equations (on the two axes the face spans respectively), of the form Equation 3. After the arc splitting step, each inner loop at most provides 1 equation (on the axis the two added arcs belong to). But there is one redundant equation on each axis. So there are at most $2|P| + k - 3$ independent equations provided by patches. Another part of equations comes from homology basis of the *polycube graph*, of the form Equation 4. There are $2g$ loops in the homology basis. Every loop spans all three axes, so all loops provide at most $6g$ independent equations. In total, there are at most $2|P| + k - 3 + 6g$ independent equations in the linear system. The number of variables is $|A'|$. Thus, according to Equation 9 and Equation 6, the kernel dimension of the linear system would be $|P| - 3$. All shape spaces in our extensive experiments achieve exactly $|P| - 3$ dimensions.
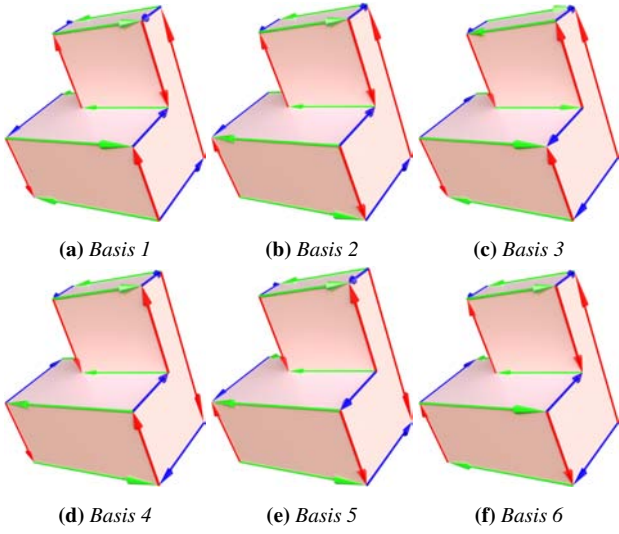
(a) *Basis 1*   **(b)** *Basis 2*   **(c)** *Basis 3*

(d) *Basis 4*   **(e)** *Basis 5*   **(f)** *Basis 6*

Figure 16: *The basis of the* polycube shape space *for the "duck" mesh and a* polycube graph. *The directions of the basis are with respect to the initial assignment.*

5. Polycube Embedding

Let $\Omega = \{\omega^1, \omega^2, \ldots, \omega^n\}$ denote the basis of a *polycube shape space*. Every *exact* and *closed* differential one-form ω can be expressed as a linear combination of the basis ω^i as the following:

$$\omega = \sum_{\omega^i \in \Omega} c_i \cdot \omega^i, \tag{10}$$

where c_i is the weight coefficient of the linear combination.

Assume ω has a valid polycube embedding, let V_ω denote the set of vertex positions of that embedding, then V_ω must be able to be realized in $\mathbb{R}^3$ space by integrating ω, i.e., a 0-form. Every basis ω^i induces a 0-form V_{ω}^i, which has value $V_{\omega^i}(v_j)$ on a vertex v_j. We call $V_\Omega = \{V_{\omega^1}, V_{\omega^2}, \ldots, V_{\omega^n}\}$ as the basis of all 0-forms.

The 0-form $V_\omega(v_j)$ can be expressed by a linear combination of the basis of V_Ω:

$$V_\omega(v_j) = \sum_{V_\Omega} c_i V_{\omega^i}(v_j) = \sum_{\omega^i \in \Omega} c_i \omega^i(v_j) = \sum_{\omega^i \in \Omega} c_i \int_{v_0}^{v_j} \omega^i, \tag{11}$$

where the root vertex v_0 has the position $(0, 0, 0)$.

Each element of the *polycube shape space* corresponds to a 0-form. But not all of them can be embedded in $\mathbb{R}^3$. If a *polycube graph* is embedded on a mesh and we look for an optimal *polycube embedding* to approximate the mesh, we propose to use the positions of the nodes of a *polycube graph* embedded on the mesh as the target position $\bar{V}$, then we define a *polycube energy* E_p as the following quadratic format to find the optimal 0-form V_o:

$$E_p = (V_o - \bar{V})^2 = (\sum_{\omega^i \in \Omega} c_i \cdot \int \omega^i - \bar{V})^2 \tag{12}$$

The optimal solution V_o, i.e., the optimal *polycube polyhedron*, approximates the target $\bar{V}$ closely, i.e., the original mesh, as shown in Fig. 17. There are six optimal solutions corresponding to six

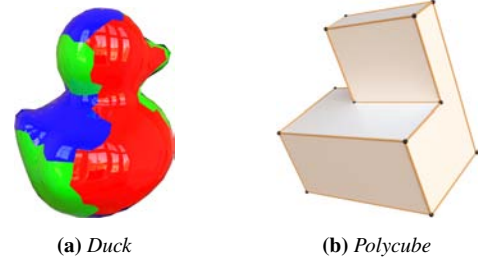color schemes, we choose the one with the smallest energy error as our result.

(a) *Duck*   **(b)** *Polycube*

Figure 17: *The "duck" model and its optimal polycube polyhedron.*

5.1. Prescribed Constraints.

Our method has a special feature in generating the *polycube polyhedron*. We can add edge length constraints in the energy system, as shown in Fig. 18. Since we do not know the edge directions before embedding, we adjust the edge length values after embedding and reconstruct the *polycube embedding*. For example, after the first embedding, we get the length value of the arc a_i as $L_i = l_i$, then we can add the following constraint to modify this edge length by scalar k:

$$L_i = k l_i, \tag{13}$$

we can also change its direction:

$$L_i = -l_i. \tag{14}$$

(a)   **(b)**   **(c)**
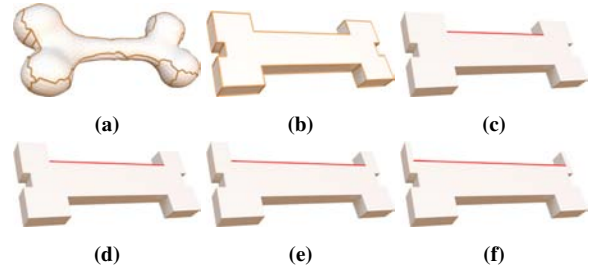
(d)   **(e)**   **(f)**

Figure 18: *The* polycube embeddings *with the four different edge length constraints (red line).*

5.2. Non-Degenerated Polycube Embedding

The *embedding* of some differential one-forms from the *polycube shape space* will produce a *degenerated polycube embedding*, which has two critical status: 1) the arcs on the same face cross each other (Fig. 19); 2) a face intersects with another non-neighboring face, i.e., two faces are tangent to each other.

The first critical status can be expressed as the linear equality:

$$L_i = 0. \tag{15}$$

The second critical status can be expressed as the linear equality:

$$(V_\omega(v_i) - V_\omega(v_j)) \cdot \mathbf{n}_i = 0, \tag{16}$$

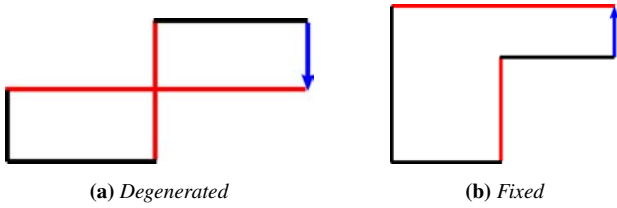**(a)** *Degenerated*   **(b)** *Fixed*

Figure 19: *The degenerated cases.*

here v_i, v_j are two vertice of face f_i, f_j respectively, and $\mathbf{n}_i$ is the unit normal vector of face f_i. This equality means that the distance between two parallel faces f_1 and f_2 is zero.

The adjacent patches in a *polycube graph* are orthogonal in the *polycube polyhedron*. If there are two faces co-planar, they must be non-adjacent patches. We treat this case to be not valid. On the other hand, the purpose of this constraint is to constrain that one face should be on the desired side of the other face. This kind of constraints is added only when we find that the change of side can eliminate face intersections.
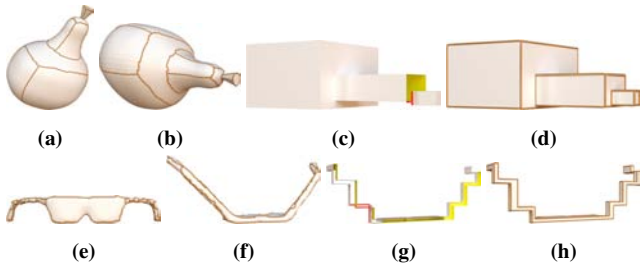

(a)   **(b)**   **(c)**   **(d)**

(e)   **(f)**   **(g)**   **(h)**

Figure 20: *The "pear" (a), (b) and "glass" (e), (f) models with two different views; the* degenerated polycube embedding *(c), (g); the* fixed polycube embedding *(d),(h).*

An optimal *polycube polyhedron* without degeneration (Fig. 20) can be constructed by solving a system of quadratic optimization with linear inequality constraints.

$$\text{minimize } E_p = (V_o - \bar{V})^2 = (\sum_{\omega^i \in \Omega} c_i \cdot \int \omega^i - \bar{V})^2$$

subject to

$$L_i \geq \varepsilon, \text{ or}$$
$$L_i \leq -\varepsilon, \text{ or}$$
$$(V_\omega(v_i) - V_\omega(v_j)) \cdot \mathbf{n}_i \geq \varepsilon, \text{ or}$$
$$(V_\omega(v_i) - V_\omega(v_j)) \cdot \mathbf{n}_i \leq -\varepsilon$$

where ε is the smallest allowed edge length.

Interactive user interface [LS07] is proved to be a useful tool in graphic applications. We also use an interactive user interface to set up the unknown inequality value by visualization of the resutls and update the *degenerated polycube embedding* to a valid one. Since each *polycube graph* already has an embedding in the original mesh, in our experiment, such adjustment rarely happens.

(a) *Airplane*   **(b)** *Airchair*   **(c)** *Armadilo*

Figure 21: *The polycube polyhedra of some meshes of genus zero.*

(a) *Botijo*   **(b)** *Dancing children*   **(c)** *Elk*

Figure 22: *The polycube polyhedra of some meshes of the high genus.*

We demonstrate the applicability of our *polycube embedding* algorithm with dozens of varying meshes, some are exhibited in Fig. 21 and Fig. 22. Since our algorithm is based on a linear system, it is very fast. Our experiments show that our method is robust to the meshes of different genus and geometries.

6. Applications

In this section, we demonstrate that our framework of *polycube shape space* can be applied in the applications of *polycube mesh*, quadrangulation [BZK09; BLP*13] and all-hex meshing [HJS*14; FBL16].

6.1. Polycube Mesh

Different from previous deformation based methods, we propose a graph-based approach to create a bijective cross-mapping *polycube mesh* (Fig. 27) by parameterizing a mesh *M* onto the *polycube polyhedron* generated from an input *polycube graph*. We call it *polycube parameterization* (Fig. 23), which consists of three steps: 1)

the nodes of the *polycube graph* are mapped to the nodes of the *polycube polyhedron*; 2) the vertices on the arcs of the *polycube graph* are mapped onto the edges of the *polycube polyhedron* according to their length ratio (Fig. 23b); 3) every patch of the mesh separated by the *polycube graph* are parameterized onto the corresponding face of *polycube polyhedron* by some fixed-boundary bijective parameterization [FL16] (Fig. 23d).
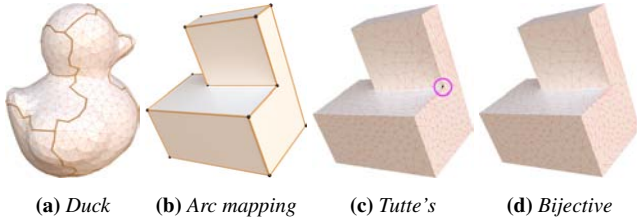

(a) *Duck*   **(b)** *Arc mapping*   **(c)** *Tutte's*   **(d)** *Bijective*

Figure 23: *The triangles in the "orange" circle have flips.*

Every patch can apply different parameterization algorithms independently. If a patch has four arcs and is simply connected, we use Tutte's embedding algorithm [Flo03; GGT06] to obtain a bijective result. When a patch has more than four arcs, it may not have a convex boundary and maybe non-simply connected. Therefore the Tutte's method cannot guarantee a bijective result [FP06] (Fig. 23c), we apply the optimization methods in [FL16; AL13] to obtain a bijective mapping (Fig. 23d). It is possible to obtain a better bijective cross-mapping with lower distortion by adjusting the prescribed edge lengths to change the shape of the *polycube polyhedron*.
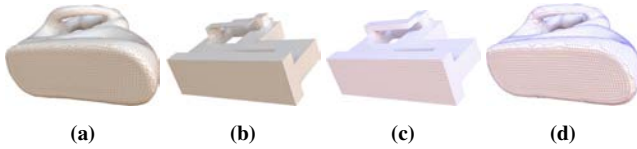

(a)   **(b)**   **(c)**   **(d)**

Figure 24: *The original triangular mesh (a), its bijective cross-mapping* polycube mesh *(b), the quadrangular* polycube mesh *(c), the final quad-meshing result (d).*

6.2. Quadrangulation

Polycube mesh can be used in quadrangulation. Given a mesh and its bijective cross-mapping *polycube mesh*, first we compute a quadrangular *polycube mesh*, second, we pull it back onto the original mesh by the barycentric coordinates, as exhibited in Fig. 24. More quad-meshing results are provided in Fig. 25.

6.3. All-hex Meshing.

The all-hex meshing algorithms [GSZ11; HJS*14; FBL16] produce one single optimal *tetrahedral polycube mesh* by deforming a volume tetrahedral mesh to minimizing an energy. Our method uses a different work-flow: 1) prescribe a *polycube graph* on a surface mesh; 2) generate the tetrahedral volume mesh from a surface mesh; 3) compute the *polycube mesh* of the surface mesh; 4) map
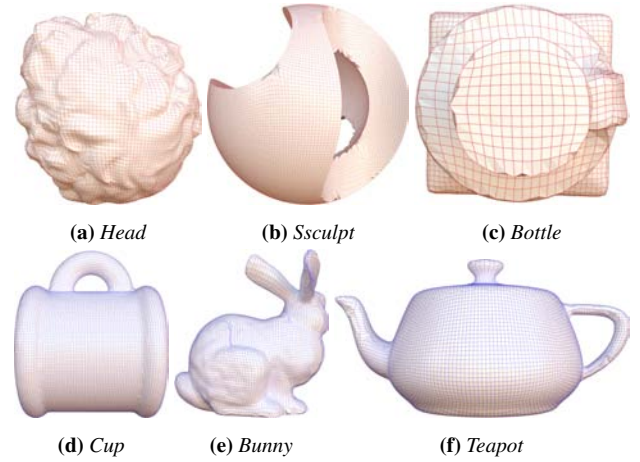

(a) *Head*   **(b)** *Ssculpt*   **(c)** *Bottle*

(d) *Cup*   **(e)** *Bunny*   **(f)** *Teapot*

Figure 25: *The quad meshing results.*

the tetrahedral mesh onto the volume of the *polycube mesh*; 5) tessellate the *polycube mesh* into a *hexahedral polycube mesh*; 6) pull back the *hexahedral polycube mesh* onto the original tetrahedral mesh with the barycentric coordinates. The work-flow is illustrated in Fig. 26.

The fourth step is a fixed boundary volume parameterization problem. We use the volumetric harmonic mapping [WGC*04] to get an initial result with flips, then an optimization method [FL16] can be applied to improve the volume mapping.
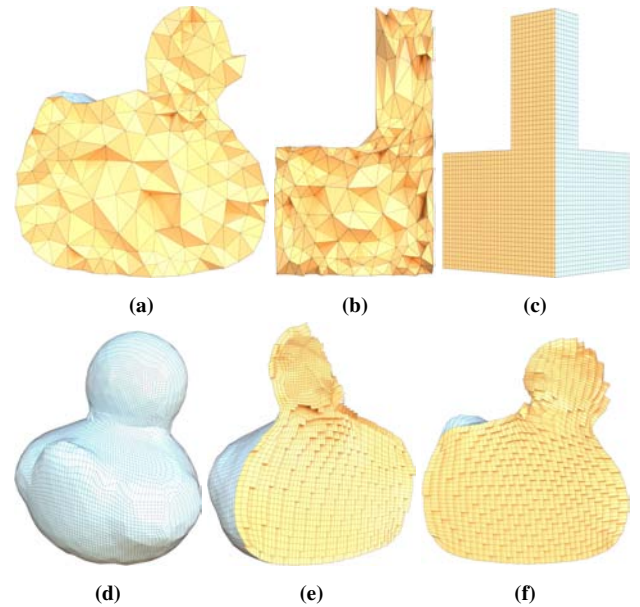

(a)   **(b)**   **(c)**

(d)   **(e)**   **(f)**

Figure 26: *The tetrahedral mesh (a); the cross-mapping tetrahedral polycube mesh (b); the hexahedral polycube mesh (c); the hex meshing result (d); the slices of the hexhedral mesh (e), (f).*
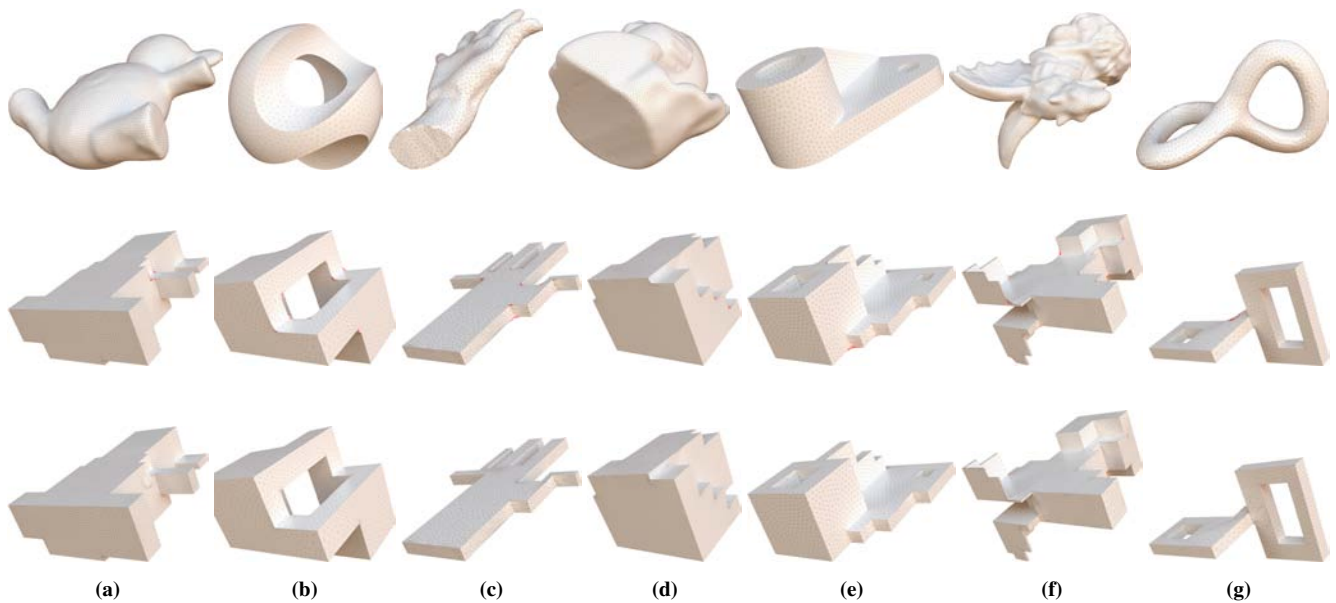
Figure 27: *The polycube meshes: the first row shows the original models; the second row exhibits the Tutte's mappings with flips (red parts), the flipped triangles are located on the reflect corners [GGT06] of the patches; the third row demonstrates the bijective results*

7. Conclusion and Future Work

In this paper, we address the graph-theoretic characterizations of the skeleton graph of *polycube polyhedron* of high-genus and non-simply connected faces. We prove the necessary condition of the *polycube graph*. Our proof is based on a linear system that illustrates the *exact* and *closed* differential one-form. We conclude that if a *polycube graph* has more than 3 patches, i.e., circles, then it could be the skeleton graph of a *polycube polyhedron*. Our proof also leads to a *polycube embedding* algorithm naturally.

Although we focus on establishing the relationship between graphs and polyhedra to generalize the Steinitz's theorem and Eppstein's theorem in this paper, we also propose a novel graph-based framework for the applications of *polycube mesh* generations, quad and hex meshing. However, our framework requires a *polycube graph* as the input. It is potential to apply some layout graph generation algorithms [CK14; EGKT08; RRP15; RP17] to find a valid graph automatically and a better embedding, which follows the feature lines of the mesh, to achieve a better result.

Acknowledgments

References

[AL13] AIGERMAN, NOAM and LIPMAN, YARON. "Injective and bounded distortion mappings in 3D". *ACM Transactions on Graphics (TOG)* 32.4 (2013), 106 10.

[BLP*13] BOMMES, DAVID, LÉVY, BRUNO, PIETRONI, NICO, et al. "Quad-Mesh Generation and Processing: A Survey". *Computer Graphics Forum*. Vol. 32. 6. Wiley Online Library. 2013, 51–76 9.

[BZK09] BOMMES, DAVID, ZIMMER, HENRIK, and KOBBELT, LEIF. "Mixed-integer quadrangulation". *ACM Transactions On Graphics (TOG)* 28.3 (2009), 77 9.

[CK14] CAMPEN, MARCEL and KOBBELT, LEIF. "Quad layout embedding via aligned parameterization". *Computer Graphics Forum*. Vol. 33. 8. Wiley Online Library. 2014, 69–81 3, 11.

[CL*10] CHANG, CHIN-CHEN, LIN, CHEN-YU, et al. "Texture tiling on 3d models using automatic polycube-maps and wang tiles". *Journal of Information Science and Engineering* 26.1 (2010), 291–305 2.

[CLS16] CHERCHI, GIANMARCO, LIVESU, MARCO, and SCATENI, RICCARDO. "Polycube Simplification for Coarse Layouts of Surfaces and Volumes". *Computer Graphics Forum*. Vol. 35. 5. Wiley Online Library. 2016, 11–20 3.

[CXW*19] CHEN, LONG, XU, GANG, WANG, SHIYI, et al. "Constructing volumetric parameterization based on directed graph simplification of L1 polycube structure from complex shapes". *Computer Methods in Applied Mechanics and Engineering* 351 (2019), 422–440 3.

[DS96] DILLENCOURT, MICHAEL B and SMITH, WARREN D. "Graph-theoretical conditions for inscribability and Delaunay realizability". *Discrete Mathematics* 161.1-3 (1996), 63–77 2.

[EGKT08] EPPSTEIN, DAVID, GOODRICH, MICHAEL T, KIM, ETHAN, and TAMSTORF, RASMUS. "Motorcycle graphs: canonical quad mesh partitioning". *Computer Graphics Forum*. Vol. 27. 5. Wiley Online Library. 2008, 1477–1486 11.

[EM10] EPPSTEIN, DAVID and MUMFORD, ELENA. "Steinitz theorems for orthogonal polyhedra". *Proceedings of the twenty-sixth annual symposium on Computational geometry*. ACM. 2010, 429–438 1, 2, 4, 6.

[FBL16] Fu, Xiaoming, Bai, Chongyang, and Liu, Yang. "Efficient Volumetric PolyCube-Map Construction". *Computer Graphics Forum (Pacific Graphics)* 35.7 (2016) 2, 3, 9, 10.

[FJFS05] Fan, Zhengwen, Jin, Xiaogang, Feng, Jieqing, and Sun, Hanqiu. "Mesh morphing using polycube-based cross-parameterization". *Computer Animation and Virtual Worlds* 16.3-4 (2005), 499–508 2.

[FL16] Fu, Xiao-Ming and Liu, Yang. "Computing inversion-free mappings by simplex assembly". *ACM Transactions on Graphics (TOG)* 35.6 (2016), 216 10.

[Flo03] Floater, Michael. "One-to-one piecewise linear mappings over triangulations". *Mathematics of Computation* 72.242 (2003), 685–696 10.

[FP06] Floater, Michael S and Pham-Trong, Valérie. "Convex combination maps over triangulations, tilings, and tetrahedral meshes". *Advances in Computational Mathematics* 25.4 (2006), 347–356 10.

[FXBH16] Fang, Xianzhong, Xu, Weiwei, Bao, Hujun, and Huang, Jin. "All-hex meshing using closed-form induced polycube". *ACM Transactions on Graphics (TOG)* 35.4 (2016), 124 3.

[GGT06] Gortler, Steven J, Gotsman, Craig, and Thurston, Dylan. "Discrete one-forms on meshes and applications to 3D mesh parameterization". *Computer Aided Geometric Design* 23.2 (2006), 83–112 10, 11.

[GKKZ67] Grünbaum, Branko, Kaibel, Volker, Klee, Victor, and Ziegler, Günter M. *Convex polytopes*. Vol. 1967. Springer, 1967 1, 2.

[GSZ11] Gregson, James, Sheffer, Alla, and Zhang, Eugene. "All-Hex Mesh Generation via Volumetric PolyCube Deformation". *Computer graphics forum*. Vol. 30. 5. Wiley Online Library. 2011, 1407–1416 2, 3, 10.

[GXH*13] Garcia, Ismael, Xia, Jiazhi, He, Ying, et al. "Interactive applications for sketch-based editable polycube map". *Visualization and Computer Graphics, IEEE Transactions on* 19.7 (2013), 1158–1171 2.

[HJS*14] Huang, Jin, Jiang, Tengfei, Shi, Zeyun, et al. "L1-Based Construction of Polycube Maps from Complex Shapes". *ACM Transactions on Graphics (TOG)* 33.3 (2014), 25 2, 3, 9, 10.

[Hon08] Hong, Seok-Hee. "Extending Steintz' theorem to Non-convex Polyhedra". *Tech. Rep. 2008-012, Department of Applied Mathematics and Physics, Kyoto University* (2008). http://www.amp.i.kyoto-u.ac.jp/tecrep/abst/2008/2008-012.html 2.

[HRS92] Hodgson, Craig D, Rivin, Igor, and Smith, Warren D. "A characterization of convex hyperbolic polyhedra and of convex polyhedra inscribed in the sphere". *Bulletin of the American Mathematical Society* 27.2 (1992), 246–251 2.

[HTWB11] Huang, Jin, Tong, Yiying, Wei, Hongyu, and Bao, Hujun. "Boundary aligned smooth 3D cross-frame field". *ACM transactions on graphics (TOG)*. Vol. 30. 6. ACM. 2011, 143 2, 3.

[HWFQ09] He, Ying, Wang, Hongyu, Fu, Chi-Wing, and Qin, Hong. "A divide-and-conquer approach for automatic polycube map construction". *Computers & Graphics* 33.3 (2009), 369–380 3.

[HXH10] Han, Shuchu, Xia, Jiazhi, and He, Ying. "Hexahedral shell mesh construction via volumetric polycube map". *Proceedings of the 14th ACM Symposium on Solid and Physical Modeling*. ACM. 2010, 127–136 2.

[Jak10] Jakob, Wenzel. *Mitsuba renderer*. http://www.mitsuba-renderer.org. 2010 11.

[JHW*14] Jiang, Tengfei, Huang, Jin, Wang, Yuanzhen, et al. "Frame field singularity correctionfor automatic hexahedralization". *IEEE Transactions on Visualization and Computer Graphics* 20.8 (2014), 1189–1199 2, 3.

[LBK16] Lyon, Max, Bommes, David, and Kobbelt, Leif. "HexEx: robust hexahedral mesh extraction". *ACM Transactions on Graphics (TOG)* 35.4 (2016), 123 2, 3.

[LJFW08] Lin, Juncong, Jin, Xiaogang, Fan, Zhengwen, and Wang, Charlie CL. "Automatic polycube-maps". *Advances in Geometric Modeling and Processing*. Springer, 2008, 3–16 3.

[LLX*12] Li, Yufei, Liu, Yang, Xu, Weiwei, et al. "All-hex meshing using singularity-restricted field". *ACM Transactions on Graphics (TOG)* 31.6 (2012), 177 2.

[LS07] Lipson, Hod and Shpitalni, Moshe. "Optimization-based reconstruction of a 3D object from a single freehand line drawing". *ACM SIGGRAPH 2007 courses*. ACM. 2007, 45 9.

[LVS*13] Livesu, Marco, Vining, Nicholas, Sheffer, Alla, et al. "PolyCut: Monotone Graph-Cuts for PolyCube Base-Complex Construction". *Transactions on Graphics (Proc. SIGGRAPH ASIA 2013)* 32.6 (2013). DOI: 10.1145/2508363.2508388 2–4.

[LZLW15] Liu, Lei, Zhang, Yongjie, Liu, Yang, and Wang, Wenping. "Feature-preserving T-mesh construction using skeleton-based polycubes". *Computer-Aided Design* 58 (2015), 162–172 2.

[NRP11] Nieser, Matthias, Reitebuch, Ulrich, and Polthier, Konrad. "Cubecover–parameterization of 3d volumes". *Computer Graphics Forum*. Vol. 30. 5. Wiley Online Library. 2011, 1397–1406 2.

[Riv96] Rivin, Igor. "A characterization of ideal polyhedra in hyperbolic 3-space". *Annals of mathematics* 143.1 (1996), 51–70 2.

[RP17] Razafindrazaka, Faniry H and Polthier, Konrad. "Optimal base complexes for quadrilateral meshes". *Computer Aided Geometric Design* 52 (2017), 63–74 11.

[RRP15] Razafindrazaka, Faniry H, Reitebuch, Ulrich, and Polthier, Konrad. "Perfect matching quad layouts for manifold meshes". *Computer Graphics Forum*. Vol. 34. 5. Wiley Online Library. 2015, 219–228 11.

[THCM04] Tarini, Marco, Hormann, Kai, Cignoni, Paolo, and Montani, Claudio. "Polycube-maps". *ACM Transactions on Graphics (TOG)* 23.3 (2004), 853–860 2, 3.

[WGC*04] Wang, Yalin, Gu, Xianfeng, Chan, Tony F, et al. "Volumetric harmonic brain mapping". *Biomedical Imaging: Nano to Macro, 2004. IEEE International Symposium on*. IEEE. 2004, 1275–1278 10.

[WJH*08] Wang, Hongyu, Jin, Miao, He, Ying, et al. "User-controllable polycube map for manifold spline construction". *Proceedings of the 2008 ACM symposium on Solid and physical modeling*. ACM. 2008, 397–404 2, 3.

[YL08] Yao, Chih-Yuan and Lee, Tong-Yee. "Adaptive geometry image". *Visualization and Computer Graphics, IEEE Transactions on* 14.4 (2008), 948–960 3.

[Zie12] Ziegler, Günter M. *Lectures on polytopes*. Vol. 152. Springer Science & Business Media, 2012 1, 2.

[ZLL*18] Zhao, Hui, Lei, Na, Li, Xuan, et al. "Robust edge-preserving surface mesh polycube deformation". *Computational Visual Media* 4.1 (2018), 33–42 3.